

Measurements of early time radiation asymmetry in vacuum and methane-filled *Hohlraums* with the reemission ball technique

G. R. Magelssen, N. D. Delamater, E. L. Lindman, and A. A. Hauer

Los Alamos National Laboratory, Los Alamos, New Mexico 87544

(Received 12 November 1996; revised 15 September 1997)

In a previous paper [Phys. Rev. E **53**, 5240 (1996)], we presented experimental results of a technique for measuring time resolved symmetry in vacuum *Hohlraums* irradiated with the laser beams from the NOVA laser located at Lawrence Livermore National Laboratory. The experimental method involved x-ray imaging a high-Z ball placed in the center of a laser irradiated vacuum *Hohlraum*. The signal from the high-Z ball was measured along the *Hohlraum* axis, and compared with calculations. In this paper, using this experimental technique, we present time-dependent reemission measurements and calculations of the drive symmetry in vacuum and methane-filled *Hohlraums* for a shaped laser pulse. We also present a method for determining the time dependence of the radiation flux from the measured reemission signal ratios, and do a modal analysis to determine the values of the dominant Legendre components. [S1063-651X(98)06304-1]

PACS number(s): 52.25.-b

I. INTRODUCTION

Understanding and controlling symmetry in indirect drive is critical to achieving the high convergence ratios needed for significant gain from capsule implosions [1–5]. Over the last few years much effort and progress has been made in measuring and understanding symmetry within *Hohlraums* [6,7]. By imaging the compressed cores of imploded capsules, time integrated estimates of the symmetry have been made in vacuum as well as methane-filled *Hohlraums*. This technique has been applied in a couple of different ways. The first method that will be referred to as the “standard capsule” technique uses a NOVA plastic (CH) capsule which has a shell thickness of 55 μm and an inner radius of 220 μm . The capsule fill pressure is 50 atm of deuterium, and 1/10 atm of argon. The imploded core image is the result of the symmetry occurring throughout the capsule implosion, a time of 2.2 and 2.5 ns for the shaped laser pulse used in many experiments. It is a time integrated image [8–11]. The second method, that will be referred to as the “symmetry capsule” technique, uses earlier time sampling by thinning the capsule shell to create an implosion at an earlier time. Typically, the shell thickness is about 20 μm . The deuterium pressure inside the shell is about 6 atm to maintain a convergence ratio (initial to final capsule radius) of about 8, the same as a standard capsule. Also, the argon pressure is about 1 atm to achieve a good x-ray signal. Because the implosion occurs at an earlier time, the imploded core image is a measure of the symmetry integrated over this reduced implosion time period. This has resulted in measurements of the time integrated symmetry for the first ns of the PS22 laser pulse (Fig. 1), a 1:3 power ratio laser pulse [12].

Two other methods use the motion of specific emission regions to study symmetry. One method looks directly at the laser spot emission in low energy x rays by observing through a large slit in the *Hohlraum* wall. Symmetry is studied by tracking the motion of the laser emission region in three different x-ray energy channels [13]. The other method images laser spot emission through a two micron gold *Hohl-*

raum wall with a 100–150- μm outer CH layer. Symmetry is studied by measuring the motion of the x rays from the hot x-ray ring created by the laser spots [14]. For this paper this method will be referred to as the “thin-wall hohlraum” technique.

Another method that uses x-ray backlighting places a foam ball in the capsule location inside of the *Hohlraum*. Measurements of the location of the shock front are made as a function of time. This is done by backlighting the ball with an appropriate x-ray spectrum as the foam ball implodes. The measured distortion in the shock front is used to infer the asymmetry [15].

In this paper, we present results using the reemission technique to obtain drive symmetry measurements in vacuum and methane-filled *Hohlraums* at NOVA. The experimental technique involves imaging a Bi ball placed in the center of a laser irradiated *Hohlraum*. As described in our earlier paper

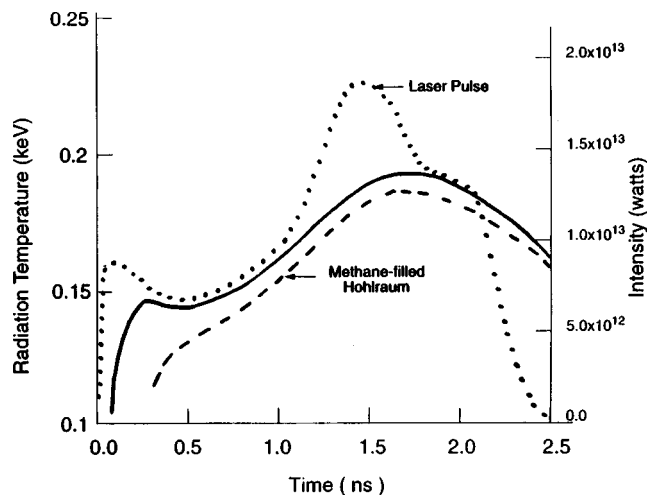


FIG. 1. A typical PS22 laser power pulse is depicted. Also shown are radiation temperature profiles for vacuum and methane-filled *Hohlraums* that were irradiated with a PS22 laser pulse. The measurements are for *Hohlraums* without a capsule which is the typical method for making these measurements.

[1], after about 1 ns; the gold plasma blowoff from the *Hohlraum* wall collides with the bismuth plasma from the reemission ball. This collision causes x-ray emission from the ball region. Because this emission is not directly related to the x-ray flux incident on the ball, the method is limited to measuring symmetry at early time, and for this paper to times less than 1 ns. Measurements and calculations of the pole (along the *Hohlraum* axis) to equator (perpendicular to the *Hohlraum* axis) signal ratio in vacuum and methane-filled *Hohlraums* will be presented. We also present a method for determining the time dependence of the radiation flux from the measured signal ratios, and do a Legendre modal analysis to find the time dependence of the P_1 , P_2 , and P_3 Legendre moments. For this paper, the polar and equatorial axes are defined to be along and perpendicular to the *Hohlraum* axis, respectively.

II. EXPERIMENTAL CONCEPT AND DESIGN

The reemission ball is a nonimploding solid bismuth ball positioned at the center of a *Hohlraum*. The ball is placed at the initial position of a typical imploding capsule, and samples the drive pattern at this location. The ball reemits thermal radiation under the influence of the radiation drive in the *Hohlraum*. The radiation symmetry at the ball is studied by imaging this thermal radiation reemitted from the bismuth. In a previous paper [1], we addressed many of the issues related to the reemission ball concept. For example, issues such as appropriate filtering, fluorescence, timing limitations, *Hohlraum* environment and plasma filling, target mounting mechanism, LTE (local thermodynamic equilibrium) versus NLTE (nonlocal thermodynamic equilibrium), and simple theoretical-experimental comparisons were examined. These feasibility experiments were done with a 1-ns flattop laser pulse that generated a *Hohlraum* radiation temperature above 200 eV for all but the first 200–300 ps. These experiments were done with a web mounting mechanism for holding the Bi ball.

In this paper we show that the technique can be used in a lower temperature *Hohlraum* environment in both vacuum and methane-filled *Hohlraums*, and provides early time drive symmetry measurements not available with other methods. The experimental results presented used the shaped laser pulse, PS22, with a foot-to-peak power ratio of 1:3 [2]. Our measurements occurred during the foot of this pulse where the *Hohlraum* radiation temperature varied from a 100 to 160 eV over a 1-ns duration. Because of difficulties with the web mounting mechanism it was replaced with a 7 μm diameter carbon stalk that was attached to the inner *Hohlraum* wall. It was positioned so as not to interfere with our measurement of the ball signal seen perpendicular to the *Hohlraum* axis. The carbon stalk was used for all the experiments presented.

An example of the methane-filled *Hohlraum* target configuration used in our experiments is shown in Fig. 2. The *Hohlraum* length varied from 2400 to 2800 μm , and had a 800- μm radius. The laser entrance holes had a 600- μm radius, and the *Hohlraum* walls were 25 μm thick. On each side of the *Hohlraum*, five laser beams entered the *Hohlraum* through the entrance holes and created a five spot ring pattern on the *Hohlraum* walls. The reemission ball was placed in the center of the *Hohlraum*, replacing the standard

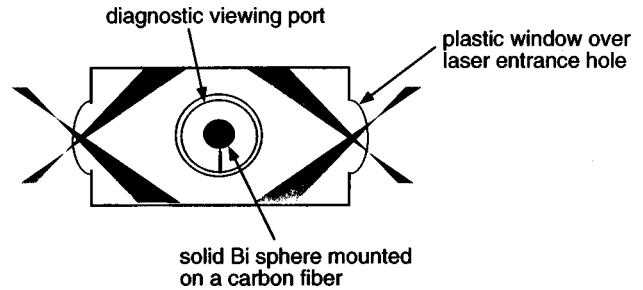


FIG. 2. Target configuration for gas-filled *Hohlraum*. Time gated x-ray imagers look both perpendicular to (through the diagnostic holes) and along (through the laser entrance holes) the *Hohlraum* axis. The diagnostic and laser entrance holes are covered with 0.35 μm of polyimide, and the *Hohlraum* is filled with 1 atm of methane.

550- μm diameter plastic capsule. The ball was solid bismuth 275–320 μm in diameter. The diagnostic hole viewing perpendicular to the *Hohlraum* axis was 700 μm in diameter to allow a good image of the bismuth ball for at least 1 ns. The emission from laser spots, the most intense source of x rays above a keV inside the *Hohlraum*, can interfere with the ball image. To eliminate the laser spot problem, a 800- μm diameter hole was placed opposite the 700- μm viewing port. In the methane-filled *Hohlraums*, the laser entrance holes and diagnostic ports were covered with 0.35 μm of polyimide, a plasticlike material, and the *Hohlraums* were filled with 1 atm of methane shortly before (a few minutes to a half hour) they were shot. As in our previous experiments, we used a 150- μm Be filter which gives a transmission peak between 2 and 3 keV. The lasers were pointed so that the center point where the five NOVA laser beams crossed was located along the *Hohlraum* axis at the laser entrance hole.

Previous experiments used a beam imbalance along the polar axis to address the methods potential for measuring symmetry. For example, five beams on one side were given higher power than those on the other. The beam imbalance caused a measurable P_1 Legendre mode from the bismuth ball. Measurements with typical time-gated images and theoretical comparisons were presented in our previous paper [1]. The experiments presented here concentrate on the pole-to-equator asymmetry, a P_2 Legendre mode. As demonstrated in implosion experiments [6–7], moving the five beam laser bundles along the *Hohlraum* axis changes the drive on the capsule from pole hot (beams outward near the laser entrance holes) to equator hot (beams inward near the capsule). When the laser beams all cross at the laser entrance hole, this symmetry control can also be achieved by changing the *Hohlraum* length [2]. For example, for vacuum *Hohlraums* like the ones used in our experiments, a *Hohlraum* length of 2800 μm creates a pole hot drive, while a length of 2400 μm creates an equator hot drive. For the experiments presented, the latter technique is used. The *Hohlraum* length was varied from 2400 to 2800 μm . To achieve more accurate measurements of the pole-to-equator symmetry, restrictions were placed on the beam-to-beam energy balance and on the power balance. The beam-to-beam energy rms was less than 5%. The laser power balance during the foot was about 10% rms, and during the peak about 5% rms.

As in previous experiments [1], the x-ray image of the ball was measured using the gated x-ray imager (GXI) developed at Los Alamos [16–18]. The GXI is a gated microchannel plate, multiple pinhole camera with both time and space resolution. The gating of the microchannel plate pro-

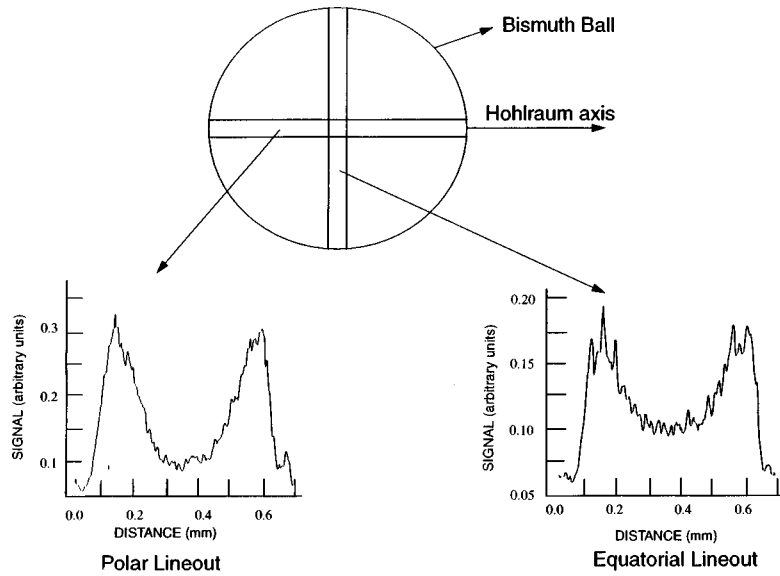


FIG. 3. Typical polar and equatorial 50- μm -wide linescans for a reemission ball.

duces a series of snapshot frames of about 80-ps duration. For our shots the temporal resolution was about 80 ps, the time gate for GXI, and the spatial resolution was about 20 μm . The x-ray pinholes were 20 μm in diameter. The GXI camera was pointed perpendicular to the *Hohlraum* axis, and viewed through the 700- μm -diameter diagnostic hole.

The *Hohlraum* was illuminated with the ten NOVA beams using the PS22 laser pulse with 25–28 kJ of laser energy. Time resolved x-ray images of the ball in the direction perpendicular to the *Hohlraum* axis were obtained from the GXI data. The images were analyzed using the data analysis code PDSHRINK [19]. The raw film density data was converted to exposure using a calibrated wedge. The image in exposure units was then filtered by a median filter to eliminate noise spikes introduced from the microchannel plate in the GXI. By taking polar and equatorial linescans through the center of each image, the pole-to-equator signal ratio was obtained and was plotted as a function of time. Furthermore, by taking azimuthal linescans, about 50 μm in width along the edge of the Bi ball, a Legendre analysis of the time dependence of P_1 , P_2 , and P_4 was done.

III. THEORETICAL MODELING

As in our previous paper two-dimensional (2D) LASNEX [20] was used to study the relationship between the reemitted image from the ball and the incident radiation flux. The following calculations were not used to compare directly to experimentally measured signals. More detailed calculations will be described later. The calculations described in this section included only the bismuth ball, a vacuum region surrounding the ball, and a boundary. As in our earlier work, NLTE radiation physics was used for the ball. A constant pole-to-equator radiation flux asymmetry, a P_2 mode, was applied at the boundary. The ball's emitted radiation and hydrodynamics were studied as a function of time for different constant values of the radiation source.

With these calculations we address three important issues

related to the emitted signal. They are the signal's uniqueness, temperature, and spectral dependence. We show that a constant radiation P_2 flux asymmetry gives rise to a unique emitted signal. We illustrate how the emitted signal depends on the incident radiation temperature. We determine that the emitted signal can be represented by a blackbody radiation emitter.

We process our calculations by a method analogous to the technique used to process the experimental data. The first step is to post process the LASNEX calculations. The post processor uses a sequence of snapshots, typically 10–20 ps apart, from a LASNEX calculation. For each snapshot the post processor does a detailed ray-trace radiation transport calculation from the ball to a specified detector. Experimentally, the x-ray camera has an exposure time (gate time) and a filter. For example, our experimental camera has an 80-ps gate time and a 150- μm Be filter. For our calculations, we used a 100-ps gate time and a flat filter that allowed all photons above 2 keV to produce the image. This filter gave about the same result as the experimental one. Polar and equatorial linescans about 50 μm wide were used to monitor the emitted radiation. Figure 3 gives an example of a typical polar and equatorial linescan. Notice that the linescans peak in intensity near the edge of the ball. This effect is due to limb brightening. The difference in the peak equatorial and polar signals is indicative of the amount of P_2 mode asymmetry. We use the ratio of these two peaks to monitor the asymmetry.

To study the uniqueness of the signal for a given incident P_2 flux asymmetry, we used an average constant value of 125 eV for the temperature source. The source was frequency dependent and came from a LASNEX calculation. Using the method described above, the pole-to-equator signal ratio was calculated as a function of time for different source asymmetries. We found that after a 100 ps the signal ratio was constant to within a couple of percent for 1 ns. For example, at an average temperature of 125 eV and a P_2 source asymmetry of 5%, 10%, and 15% (pole hot), the pole-

to-equator signal ratio was constant and equal to 1.25, 1.5, and 1.8, respectively. During the first 100 ps the albedo of the bismuth changes rapidly, and typically gives a higher signal than the value that follows. As a result, interpretation of the symmetry from the ball signal is difficult during this time.

To understand the temperature effect on the signal, the PS22 laser source was used. This source was frequency and time dependent. It was created by doing a 2D LASNEX *Hohlraum* calculation without the ball with 25 kJ of laser energy. An example of this laser profile is shown in Fig. 1. A constant 10% P_2 (pole hot) asymmetry was used for the source. The calculated signal ratio was again processed using the experimental technique described above. Ignoring the first 100 ps, we found that the signal ratio was not constant. The signal ratio does depend on the *Hohlraum* radiation temperature. At an early time when the temperature was 100 eV, the signal ratio was 1.6. At a later time when the temperature was 160 eV, the signal ratio was 1.35.

Because it was a small effect for the radiation profiles used in our previous work, we ignored signal ratio changes due to radiation temperature changes. However, as we have just shown, the emitted signal ratio from the Bi ball does depend on the radiation temperature. If we assume that the Bi ball emits like a blackbody radiator we can estimate changes in the emitted flux from changes in the *Hohlraum* radiation temperature. Consider the LASNEX calculation described above. Assume that at early time that the ball has an average temperature of 100 eV and a P_2 -like temperature gradient. Using the blackbody energy spectrum, we can calculate the energy emitted above 2 keV for different ball temperatures centered about 100 eV. For example, if the pole had a temperature of 102.4 and the equator a 100 eV, the pole-to-equator difference in photon energy emitted is 10%. The ratio of energy emitted at 102.4, and at 100 eV is 1.6 for a 2-keV flat filter. At a 160-eV and 10% flux difference, the signal ratio is 1.35. These values agree with the calculations described above.

Many other calculations were done to connect emitted signal ratios with incident radiation temperature. We found that a constant *Hohlraum* temperature and P_2 flux asymmetry resulted in a unique signal from the ball. Furthermore, we found that the incident flux and emitted flux can be related by assuming the Bi ball emits as a blackbody.

Assuming the bismuth ball is a blackbody emitter, we can relate incident flux asymmetry to emitted signal ratios. Figure 4 shows this relationship. The relationships shown are only valid for a 2-keV flat filter. Since the amount of photon energy and spectrum seen by the camera depends on the filter, one might expect that the signal ratio depends on the filter. This is indeed the situation. For the 100-eV example above, a 3-keV filter would result in a signal ratio greater than 2 not the 1.6 value given by the 2-keV flat filter. The 2-keV filter is equivalent to the 150- μm Be filter used in our experiments. As a result, the relationships depicted in Fig. 4 are valid for our experiments. We will illustrate how we use the experimental signal ratios to calculate the radiation flux in Sec. V.

Because the laser and temperature profiles depicted in Fig. 1 will be used in Sec. V they merit further discussion. Although detailed comparisons were not made, our calcu-

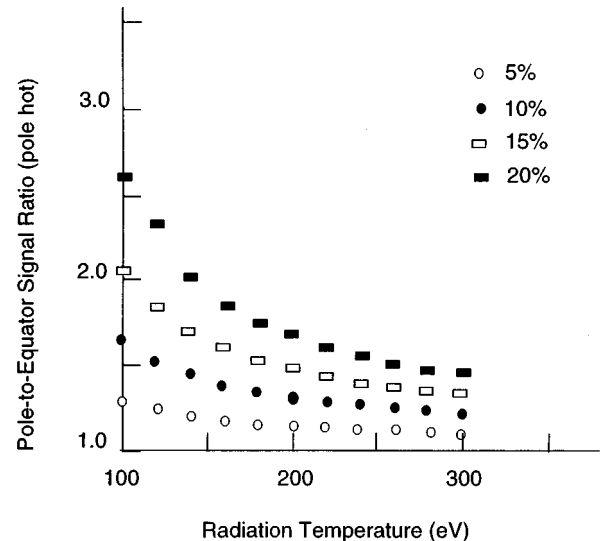


FIG. 4. Calculated relationship among radiation temperature, symmetry, and signal ratios for a filter that allows all x-rays above 2 keV to create the signal. This filter was equivalent to the 150- μm Be filter used in our experiments. The signal ratios were determined using a LTE radiation source. The four plotted curves represent 5%, 10%, 15%, and 20% radiation flux asymmetries.

lated radiation profiles are consistent with the measured vacuum and methane profiles shown in Fig. 1. These measurements were made for *Hohlraums* without a capsule [21] under conditions similar to those of our experiments. Suter *et al.* made detailed comparisons between these measurements and LASNEX calculations, and found good agreement [22]. Notice that we have ignored the effect of the ball on the radiation profile. Theoretically, we expect the capsule to have a small effect on the radiation profile, typically about a 5–10-eV drop in radiation temperature throughout time. This is because most of the radiation energy loss occurs from absorption into the *Hohlraum* walls and from loss through the laser entrance holes and diagnostic holes. Diagnostic hole losses are included in all of our calculations. For a discussion of *Hohlraum* energetics and the effect of the capsule, see the papers by Rosen [23,24].

As was discussed earlier, to measure the x-ray emission from the Bi ball requires diagnostic holes in the sides of the *Hohlraum*. In a previous paper [25,26], we presented results of the diagnostic hole effect. Here we briefly review those results. Since LASNEX is a two-dimensional code, a completely integrated *Hohlraum* calculation with diagnostic holes is not possible with LASNEX. Consequently, to study this effect we used a three-dimensional radiation transport view factor code. The calculations were totally integrated including *Hohlraum*, Bi ball, laser entrance holes, diagnostic holes, and radiation emission from each of the ten laser spots. No hydrodynamic motion was allowed. However, accurate time-dependent albedos of the *Hohlraum* walls and Bi ball were used. These calculations suggested that no measurable effect would occur in our experiments for the symmetry measurements we would make perpendicular to the *Hohlraum* axis. The calculations were accurate to the few percent level, but, of course, do not have the effects of plasma motion.

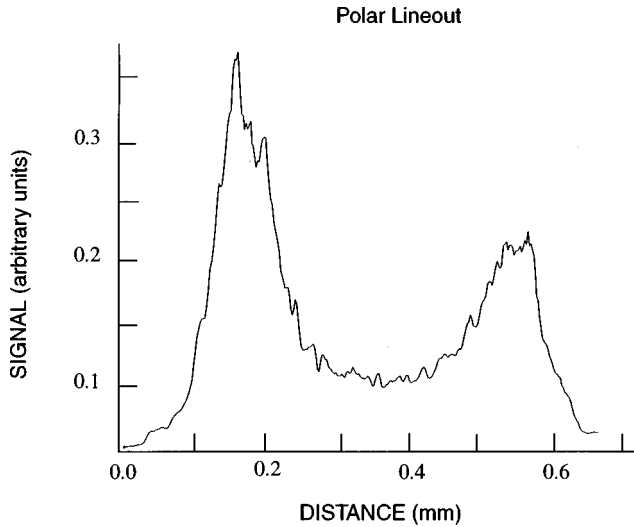


FIG. 5. Example of a polar linescan created by a pole-to-pole beam imbalance.

IV. THEORETICAL-EXPERIMENTAL COMPARISON USING SIGNAL RATIOS

A. Approach

In our previous paper we studied asymmetries along the polar axis, and made detailed comparisons between calculations and experimentally observed pole-to-pole signal ratios. Here we study the pole-to-equator signal ratios. Linescans $50 \mu\text{m}$ in width were taken along the polar and equatorial axes. Examples are shown in Fig. 3. If there is a power imbalance along the polar axis, the peak signal on one side will be higher than the other. This is illustrated in Fig. 5. For this situation we took the peak average. Also, sometimes there were small differences in the peaks in the equatorial direction. Again the average peak value was used. For the results presented, the peak differences were small, less than 10%.

Our theoretical approach was to use 2D fully integrated LASNEX calculations to compare with experimental results. These calculations included laser interaction with the *Hohlraum* walls, hydrodynamic motion of the walls and ball, and radiation emission and absorption everywhere within the *Hohlraum*. Two different SESAME equations of state [27] for gold were used and gave identical results. NLTE radiation atomic physics [28] was used for the wall and for the ball, using the average atom atomic physics package in LASNEX. To determine the effect of NLTE emission from the ball, integrated calculations with the *Hohlraum* walls NLTE and the ball LTE were also done. The calculated ball signals were the same for NLTE and LTE radiation physics. To obtain an image to compare with experimental results, the LASNEX results were post processed. The post processing was the same as described in Sec. III. The detector for our calculations had a filter equivalent to $150 \mu\text{m}$ of Be, the filter used in the experiment. In the Secs. IV B and IV C, we will refer to a laser pointing that is related to a particular *Hohlraum* length. For reference, laser pointings of 1175, 1275, 1325, and 1375 μm are related to *Hohlraum* lengths of 2400, 2600, 2700, and 2800 μm , respectively.

B. Vacuum *Hohlraum* results

Our first experimental data of the pole-to-equator signal ratio from vacuum *Hohlraums* were done with a web mount-

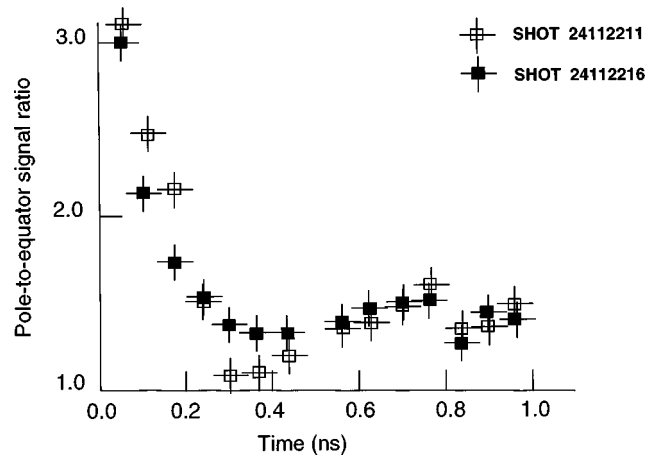


FIG. 6. Pole-to-equator signal ratios for two successive NOVA shots at a laser pointing of $1325 \mu\text{m}$ (vacuum *Hohlraums* with a length of $2700 \mu\text{m}$). The frame gate was 80 ps and the linescans $50 \mu\text{m}$ in width.

ing mechanism for holding the bismuth ball [1]. The web interfered with our measurement of the pole-to-equator signal. To avoid this problem, the web was replaced with a $7\text{-}\mu\text{m}$ C stalk oriented so as not to obscure the ball image through the diagnostic hole. All of the experimental-theoretical comparisons shown are with the stalk *Hohlraum* targets. The experimental gate time for all our measurements was 80 ps and there were 16 frames per shot covering about 1 ns of time. Because of difficulties aligning the Bi ball with the diagnostic holes and because of camera problems, typically 10–12 frames gave useful data.

To test for reproducibility, two consecutive similar shots were fired on the NOVA laser. The laser power profile and spot positions were duplicated as well as was possible. The pole-to-equator signal ratios for these two shots are shown in Fig. 6. There were slight differences in the polar beam balance on these shots, and this may have caused the slight differences in the time dependence of the signal ratios. A comparison with calculations is given in Fig. 7. The laser pointing for this experiment was $1325 \mu\text{m}$. We show two

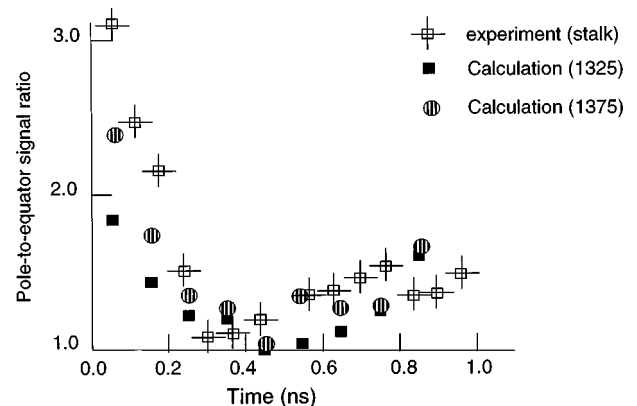


FIG. 7. Comparison between experimental and theoretical pole-to-equator signal ratios for the $1325\text{-}\mu\text{m}$ laser pointing (vacuum *Hohlraum* with a length of $2700 \mu\text{m}$). Two calculations are shown. One had a *Hohlraum* length of $2700 \mu\text{m}$, the other a length of $2800 \mu\text{m}$. Each experimental point had a 80-ps time interval and $50\text{-}\mu\text{m}$ width linescans were used.

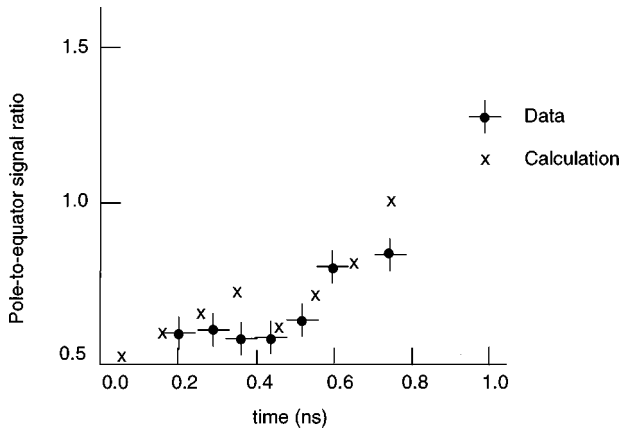


FIG. 8. Comparison between experimental and theoretical pole-to-equator signal ratios for a 1175 μm laser pointing (vacuum *Hohlraum* with a length of 2400 μm). Each experimental point had a 80-ps time interval, and 50- μm width linescans were used.

calculations, one at a pointing of 1325 μm and the other at 1375 μm . The calculation with a pointing of 1375 μm tends to agree more closely with the data, although both agree well for most of the time period. For precision NOVA measurements, the laser condition used in our experiments, it is believed that the pointing accuracy for the NOVA beams is about 30 μm . Thus this difference may be due to the pointing accuracy of the NOVA beams. The pole hot result at the 1325 pointing is in agreement with core imaging symmetry experiments done with the “standard capsule” and “symmetry capsule” techniques [6].

Our other comparison is at an inward laser pointing, 1175 μm , that should result in an equator hot asymmetry. A comparison between experiment and theory is given in Fig. 8. Again, there is close agreement between calculation and experiment. The pole-to-equator ratio is less than 1 (equator hot) over the first 800 ps. This result is consistent with “standard capsule” symmetry core imaging [6,12].

These results can best be understood by studying the effect of the placement of the laser spots, by considering changes in the wall albedos and by studying plasma flow within the *Hohlraum*. The symmetry on the ball can be made uniform at early time by the proper placement of the laser spots that create approximate rings on opposite sides of the *Hohlraum* [6,8]. With the proper location, the radiation from the rings will compensate for the nonradiating areas created by the laser entrance holes (LEH's). Early in time, before the walls have heated to any great extent, the contrast in temperature between the laser heated wall region and the other wall regions is large. If the laser ring position does not compensate for the LEH, this large contrast will give rise to large asymmetries. As a result, if the pointing is too far outward, the situation in Fig. 7, the asymmetry at early time is strongly pole hot (signal ratio greater than 1). On the other hand, if the pointing is too far inward (Fig. 8), it is strongly equator hot (a signal ratio less than 1). At intermediate times, radiation transport reduces the contrast between the wall and laser hot ring and the asymmetry is reduced (signal ratios tend toward 1). At still later times, the wall plasma flow tends to move the laser rings toward the LEH, and the symmetry becomes more pole hot. Also, the wall plasma begins to collide with the bismuth plasma from the ball. This colli-

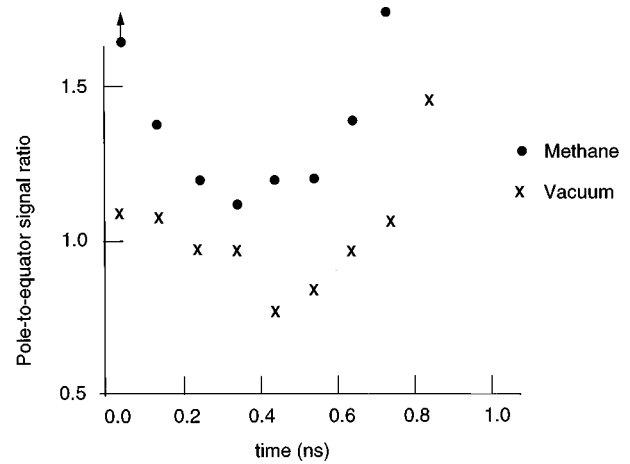


FIG. 9. Calculated difference between pole-to-equator signal ratios for vacuum and methane-filled *Hohlraums* (*Hohlraum* length was 2600 μm).

sion tends to affect the pole more than the equator for the *Hohlraum* lengths we have considered, lengths on the order of or greater than 2400 μm . The result is an artificially large signal ratio that is not related to radiation symmetry.

C. Methane-filled *Hohlraum* results

In order to reduce the laser spot motion due to plasma wall blowoff and, therefore, better control symmetry inside *Hohlraums*, the National Ignition Facility target designs have the cavity filled with a gas [29]. The gas acts to tamp the plasma blowoff. To understand the effect of the gas and the windows needed to contain the gas, a series of time-integrated symmetry shots on the NOVA laser were undertaken. Both methane- and propane-filled *Hohlraums* have been studied. These experiments were done with the PS22 laser pulse. Core imaging of implosions using the “standard capsule” technique indicate a symmetry shift from the vacuum results [4,7,9]. The data suggest a laser spot motion shift of about 150 μm toward the LEH. Similar core imaging

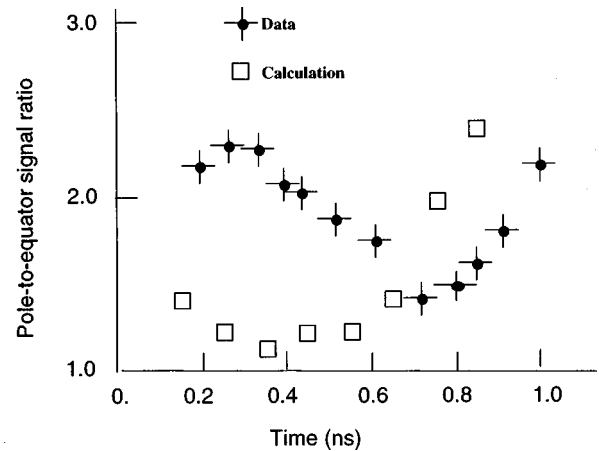


FIG. 10. Comparison between calculated and experimental pole-to-equator signal ratios for a methane-filled *Hohlraum* at a laser pointing of 1275 μm (*Hohlraum* length was 2600 μm). The time interval for each circle was 80 ps and the linescans were 50 μm in width.

using the “symmetry capsule” technique also suggests a shift toward the LEH. In this case the shift is about $90\ \mu\text{m}$ [30].

To understand the time-dependent symmetry better, we have conducted a series of reemission ball experiments in methane-filled hohlraums. The PS22 laser pulse was used. An example of the calculational symmetry difference between vacuum and methane-filled *Hohlraums* at a pointing of $1275\ \mu\text{m}$ is shown in Fig. 9. The gas-filled calculation gives a slightly higher pole hot result for all time. A comparison between experiment and theory of the pole-to-equator symmetry at a pointing of $1275\ \mu\text{m}$ is displayed in Fig. 10. One can see that calculation and experiment do not agree. In fact, the disagreement is quite large. The experiment shows a stronger pole hot asymmetry early in time. Figure 11 gives the comparison at an $1175\text{-}\mu\text{m}$ pointing. Again, the disagreement is large, and indicates a strong laser shift toward the LEH (pole hot). These experimental results are in agreement with “symmetry capsule” core imaging results [30], and “thin-wall *Hohlraum*” data of laser spot position [11].

A theory has been proposed to account for this observed “beam deflection” effect as being due to transverse plasma flow in the presence of filamentation or beam aberrations due to hot spots in the laser beam [31,32]. The effect requires both filamentation in the plasma directly heated by the laser beam and plasma material flowing at sonic velocities out the laser entrance hole transverse to the laser beam. Hot spots in the laser beams entering the *Hohlraum* create density depressions or wells in the heated plasma regions. These density wells in the filamenting plasma cause an enhanced refraction effect which deflects the laser beam toward the laser entrance hole. This plasma physics effect is not currently in our modeling codes, and limits our ability to successfully model these gas-filled *Hohlraum* experiments.

Assuming that the observed shift in symmetry is the result of beam deflection, a series of calculations was performed to try to reproduce the observed reemission ball experimental data. Because we are not aware of any calculations that can accurately predict the beam deflection for a typical unsmoothed NOVA beam profile, our calculations were not guided by theory. However, we were guided by “thin wall *Hohlraum*” imaging data [14] that suggests a $100\text{-}\mu\text{m}$ shift

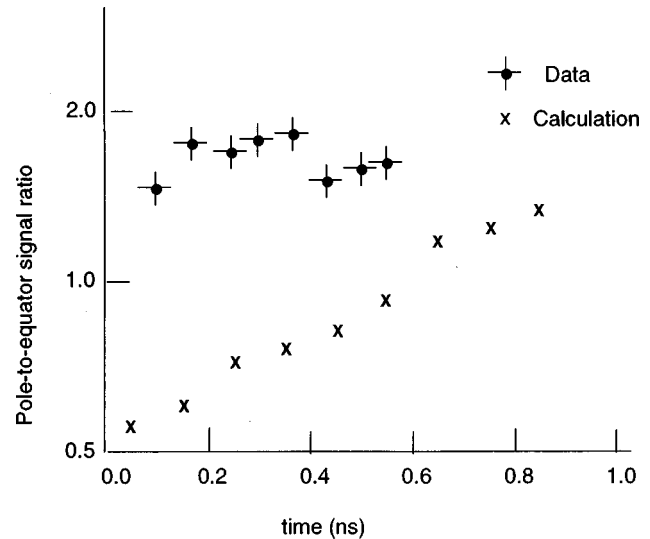


FIG. 11. Comparison between calculated and experimental pole-to-equator signal ratios for a methane-filled *Hohlraum* at a laser pointing of $1175\ \mu\text{m}$ (*Hohlraum* length was $2400\ \mu\text{m}$).

during the first 500 ps of a PS22 laser pulse and by “symmetry capsule” core imaging data that also suggests about a $100\text{-}\mu\text{m}$ shift during the first ns. For Nova measurements, the laser beams come into the *Hohlraum* at an angle 50° to the *Hohlraum* axis. An angular beam shift from 50° to 58° is about a $100\text{-}\mu\text{m}$ shift in the laser beam position on the *Hohlraum* wall. The fully integrated LASNEX calculations were done with all the physics used in previous calculations, except that the laser beam angle to the *Hohlraum* axis which would be 50° without beam deflection was allowed to vary in time. Our best calculational fit to the experimental data at a pointing of $1275\ \mu\text{m}$ is shown in Fig. 12. To obtain this result the beam laser rings were moved every 100 ps over the first 500 ps, and then did not move for the rest of the calculation. The angle of the laser ring was 50° (0–100 ps), 52° (101–200 ps), 57° (201–300 ps), 58° (301–400 ps), 56.5° (401–500 ps), and 50° thereafter. This suggests that the laser beams are shifted early in time during the first 500 ps, but then return to their original position. This laser type shift is consistent with “symmetry capsule” core imaging data [30]. Because the gold wall plasma is beginning to stagnate

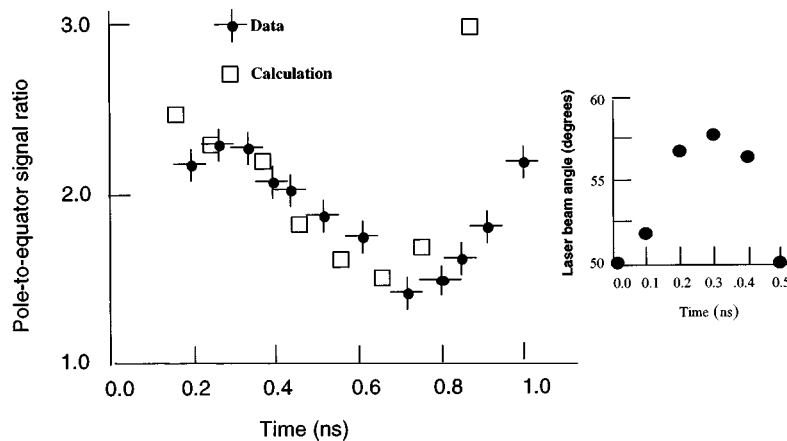


FIG. 12. Laser shift needed to reproduce the methanol-filled *Hohlraum* symmetry data at the $1275\ \mu\text{m}$ pointing. The resulting pole-to-equator signal ratio is also shown. This result was guided by thin-wall and symmetry capsule data.

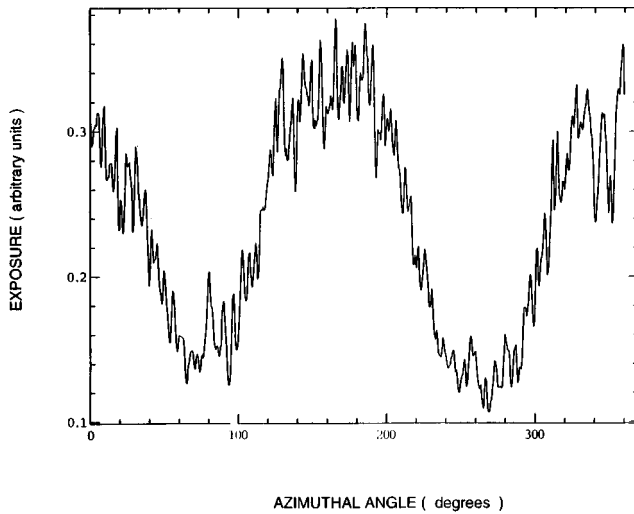


FIG. 13. An example of an azimuthal linescan from the 1275 μm laser pointing methane data. The time interval was 80 ps and this frame was about 400 ps into the laser pulse. The linescan width was 50 μm .

against the ball plasma at about 800 ps, the reemit data is suspect after 800 ps.

V. MODAL ANALYSIS—FLUX ASYMMETRY

The best method for determining the symmetry from the reemission ball signal is to use azimuthal linescans taken along the limb brightened edge of the ball. In the past this has been difficult because of camera misalignment problems. Because of this problem a large fraction of the linescan was missing, making it impossible to do an analysis in this way. As a result, pole-to-pole and pole-to-equator signal ratios were used. Our most recent experiments have allowed us to perform an azimuthal linescan analysis. A 50- μm width was chosen, and the linescans were processed using PDSHRINK with a wedge correction and median filtering. An example of the PDSHRINK linescan is shown in Fig. 13. This signal was produced in a 80-ps time interval and occurred about 400 ps into the laser pulse. The final processing step was done using MATHEMATICA software [33]. A Legendre analysis was done for every lineout not affected by misalignment or other problems. For the lineout shown in Fig. 13, the first 14 even Legendre modes are shown in Fig. 14. This is typical of the other linescans. The P_1 , P_2 , and P_4 experimental Legendre coefficients for a methane filled *Hohlraum* at a 1275- μm laser pointing is shown in Fig. 15. Error bars are not included in the figure.

Two approaches were used to determine the error associated with the Legendre coefficients of the signal. The first approach involved the method used to create the azimuthal linescans. We chose a 50- μm width because the linescans were insensitive to a plus or minus 20- μm change about this width. However, slight changes did occur. In addition, there were small uncertainties in the linescan center point. To bound the error value for P_1 , P_2 , and P_4 , 2–3 slightly different (different width or center point) azimuthal linescans were taken for each frame. The variation in the coefficients could be used to bound the signal values for the different modes. However, larger error values, the ones used here,

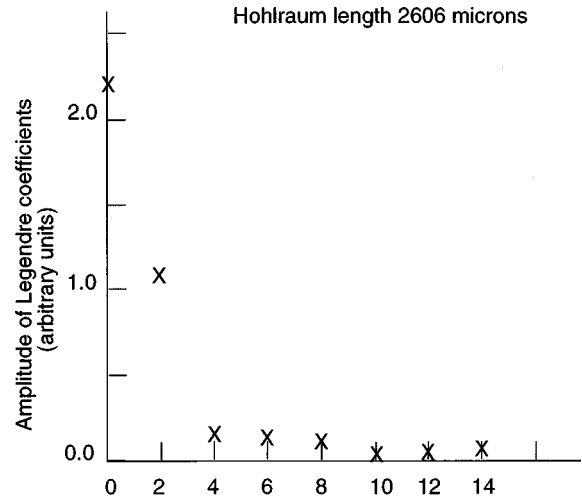


FIG. 14. Relative amplitude of the first 12 even Legendre modes for the azimuthal linescan shown in Fig. 13.

were based on the second approach.

In the second approach, a modal analysis was done for each frame giving a result similar to that shown in Fig. 14. We observed that by mode 8 the mode amplitude leveled off, and all higher modes were smaller or had roughly the same amplitude. This is indicative of the noise level in the experiment. As a result, we used this result to bound the error for the coefficients. For Fig. 14 the error amplitude is ± 0.1 , and is similar to other frames. Using this method the error in the P_1 , P_2 , and P_4 coefficients is 20%, 10%, and 25–100%, respectively. The large error for P_4 is due to the fact that at early time the coefficient was about the noise level.

There was also a timing error. The absolute timing for a NOVA laser shot is unknown to about 50–100 ps. If theory and experiment closely agree, this timing uncertainty can be reduced by aligning in time experimental and theoretical data. This was done in Figs. 6–8. Because theory and experiment disagree, this cannot be done for the results shown in Figs. 10, 11, 15, and 16.

Using the signal ratios for P_2 (Fig. 15), the radiation temperature profile for a *Hohlraum* and laser profile like this shot (Fig. 1), and the relationship between radiation temperature and signal ratio (Fig. 4), the incident radiation flux asymmetry can be estimated. The P_2 result for this shot is

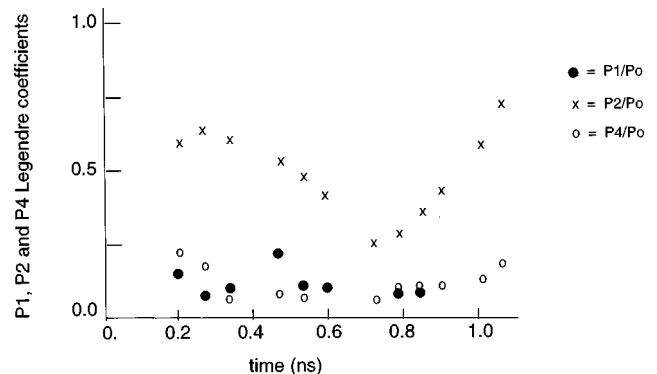


FIG. 15. P_1 , P_2 , and P_4 Legendre coefficients for the methane-filled *Hohlraum* at the 1275- μm laser pointing. Error bars are not shown but are discussed in detail in the text.

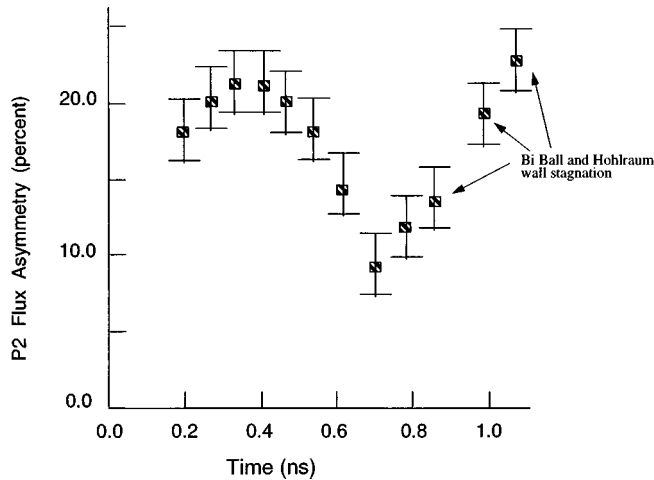


FIG. 16. Calculated P_2 flux asymmetry from the radiation temperature profile and the P_2 Legendre coefficients given in Fig. 1 and 15, respectively. There is about a 20% uncertainty in the estimated radiation flux asymmetry.

given in Fig. 16. In addition to the timing uncertainty of 50–100 ps and a signal uncertainty of 10%, there are uncertainties in the radiation temporal profile used to calculate the P_2 flux asymmetry shown in Fig. 16. Temperature measurements like that given in Fig. 1 have a 5–10 eV error bar. Further, because the temperature measurement is made without a capsule, an additional uncertainty must be added. Unlike a standard CH capsule that has a low albedo, bismuth has a very high albedo and will not affect the radiation temperature nearly as much. Our calculations suggest that the effect is less than 5 eV. Thus, the temperature error due to the bismuth ball should be small. If we assume the error in the radiation temperature is 10 eV, there is an additional 10% error in the P_2 coefficients. The signal and temperature errors combine to give a 20% uncertainty in the estimated time-dependent radiation flux asymmetry, and this is depicted in Fig. 16.

VI. CONCLUSIONS AND FUTURE PLANS

We have shown that the reemission ball design is an effective technique for measuring time resolved drive symmetry during the foot (low temperature 100–160 eV) of a laser pulse for an irradiated vacuum or methane filled *Hohlraum*.

Both azimuthal linescans and pole-to-equator signal ratios of the ball image have been shown to be effective in estimating flux asymmetries.

Detailed comparisons between calculated and experimental signal ratios indicate that we can predict the P_2 asymmetry in vacuum *Hohlraums*. However, methane-filled *Hohlraum* data does not agree with our calculations. Plasma theory [31] and simulations [32] suggest that LASNEX does not contain the necessary physics to account for the laser beam shift suggested by our methane-filled *Hohlraum* experiments. Assuming that the 90- μm shift in the symmetry capsule methane results is due to a laser pointing shift toward the LEH, the reemission data suggests that it occurs during the first 500 ps with a maximum shift angle of 8°. The laser beam movement suggested by reemission ball agrees with implosion results using “symmetry capsule” and “standard capsule” techniques [26].

We have shown that azimuthal lineouts of experimental signals allows the measurement of the P_1 , P_2 , and P_4 Legendre components of the signal ratios. We have also shown that knowledge of the *Hohlraum* radiation temperature and these signal ratios can then be used to estimate the P_1 , P_2 , and P_4 Legendre components of the radiation flux asymmetry.

Our future plans include studying the reproducibility of the P_4 results, and developing a diagnostic that incorporates features of the reemission ball and “symmetry capsule” concepts.

ACKNOWLEDGMENTS

We would like to acknowledge the LANL target fabrication group which includes L. Foreman, P. Gobby, V. Gomez, J. Moore, and K. Gifford, for their efforts in making and assembling the reemission targets. The authors acknowledge the technical assistance of S. Evans, T. Sedillo, T. Archuleta, and G. Peterson. The authors would like to acknowledge L. Suter, D. Harris, G. Pollack, and R. Turner for useful discussions on the experimental design. We also acknowledge R. Ehrlich for assistance with the production of precision energy balance on NOVA. We would also like to acknowledge the assistance of personnel at the NOVA laser facility at the Lawrence Livermore National Laboratory. This work was performed under the auspices of the U.S. Department of Energy.

[1] N. D. Delamater *et al.*, Phys. Rev. E **53**, 5240 (1996).
 [2] A. A. Hauer *et al.*, Rev. Sci. Instrum. **66**, 672 (1995).
 [3] E. L. Lindman *et al.*, in *Laser Interaction and Related Plasma Phenomena*, Proceedings of the 12th International Conference held in Osaka, Japan April 1995, edited by S. Nakai and G. Miley, AIP Conf. Proc. No. 369 (AIP, New York, 1996).
 [4] C. Stockl and G. D. Tsakiris, Phys. Rev. Lett. **70**, 943 (1993).
 [5] M. Murakami and J. Meyer-Ter-Vehn, Nucl. Fusion **31**, 1333 (1991).
 [6] A. A. Hauer *et al.*, Phys. Plasmas **2**, 2488 (1995).
 [7] N. D. Delamater *et al.*, Phys. Plasmas **3**, 2022 (1996).
 [8] L. J. Suter *et al.*, Phys. Rev. Lett. **73**, 2328 (1994).

[9] E. L. Lindman *et al.*, *Laser Interaction with Matter*, Proceedings of the 23rd European Conference, St. John’s College, Oxford, 12–13 Sept. 1994, edited by S. J. Rose, Institute of Physics Conf. Proc. No. 140 (Institute of Physics, Bristol, 1995).
 [10] N. D. Delamater *et al.*, in *Laser Interaction and Related Plasma Phenomena* (Ref. [3]), p. 95.
 [11] D. B. Harris *et al.*, Defense Res. Rev. **6**, 123 (1994).
 [12] D. B. Harris *et al.*, Bull. Am. Phys. Soc. **38**, 1885 (1993).
 [13] S. G. Glendinning *et al.* (unpublished).
 [14] N. D. Delamater *et al.* (unpublished).
 [15] Amendt *et al.*, Rev. Sci. Instrum. **66**, 785 (1995).
 [16] J. Oertel, R. E. Chrien, and J. M. Mack, in *Proceedings of the*

- 14th International Conference on Plasma Physics and Controlled Nuclear Fusion Research* (IAEA, Vienna, 1993).
- [17] J. D. Kilkenny *et al.*, Rev. Sci. Instrum. **59**, 1793 (1988).
- [18] D. K. Bradley *et al.*, Rev. Sci. Instrum. **63**, 4813 (1992).
- [19] D. W. Phillion (private communication).
- [20] G. B. Zimmerman and W. L. Kruer, Comments Plasma Phys. Control. Fusion **2**, 51 (1975).
- [21] T. J. Orzechowski, Lawrence Livermore National Laboratory Quarterly Report No. 96-3 (unpublished).
- [22] L. J. Suter *et al.*, (private communication).
- [23] M. D. Rosen (unpublished).
- [24] M. D. Rosen (unpublished).
- [25] X. Magelssen *et al.*, Defense Res. Rev. **6**, 59 (1994).
- [26] X. Magelssen *et al.*, Los Alamos National Laboratory Report No. LA-CP-93-0078, 1993 (unpublished).
- [27] G. I. Kerley, J. Chem. Phys. **73**, 469 (1980); **73**, 478 (1980).
- [28] G. Pollak (unpublished).
- [29] W. J. Krauser *et al.*, Phys. Plasmas **3**, 2084 (1996).
- [30] G. R. Magelssen *et al.*, Bull. Am. Phys. Soc. **111**, 1190 (1995).
- [31] H. A. Rose, Phys. Plasmas **3**, 1709 (1996).
- [32] E. A. Williams and D. Hinkle, Bull. Am. Phys. Soc. **111**, 1209 (1995).
- [33] S. Wolfram, *Mathematica*, 2nd ed. (Addison-Wesley, Reading, MA, 1991).